Physics of Semiconductors. Computational materials science

UDC 538.913

EDN SUQFNX
https://www.doi.org/10.33910/2687-153X-2024-5-1-30-38

Uniaxial pressure modulation of two-dimensional materials: Insights into the structure and electronic properties of $MoTe_2$ and Sb_2Te_3

R. S. Stepanov ✉ [1]

[1] Herzen State Pedagogical University of Russia, 48 Moika Emb., Saint Petersburg 191186, Russia

Author

Roman S. Stepanov, ORCID: 0000-0003-2559-7598, e-mail: stepanovroman@herzen.spb.ru

For citation: Stepanov, R. S. (2024) Uniaxial pressure modulation of two-dimensional materials: Insights into the structure and electronic properties of $MoTe_2$ and Sb_2Te_3. *Physics of Complex Systems*, 5 (1), 30–38. https://www.doi.org/10.33910/2687-153X-2024-5-1-30-38 EDN SUQFNX

Received 16 January 2024; reviewed 6 February 2024; accepted 6 February 2024.

Funding: The research was supported by the Ministry of Education of the Russian Federation as part of the state-commissioned assignment project No. VRFY-2023-0005.

Abstract. This research focuses on DFT modeling of the effects of uniaxial pressure on the electronic and structural properties of two-dimensional materials, such as $MoTe_2$ and Sb_2Te_3. Special attention is given to the reconfiguration of the van der Waals (vdW) gap. Intuitively, the application of uniaxial pressure is expected to reduce the distance between layers, leading to a transition from 2D to 3D. Investigations under uniaxial pressure on Sb_2Te_3 revealed metallization at 3 GPa. Further pressure increase induces a phase transition at 7 GPa, resulting in the disappearance of the vdW gap in the new phase. However, a transition to a bulk phase does not always occur. In the case of $MoTe_2$, pressure leads to an isostructural transition to a metallic state at 10 GPa. A further increase in pressure to 37 GPa causes a phase transition to a two-dimensional structure with a change in the orientation of the vdW gap. It is crucial to note that this $MoTe_2$ case is analogous to the situation observed in GaSe after relaxation, which is also the subject of the study.

Keywords: 2D semiconductors, van der Waals interaction, DFT, uniaxial pressure, $MoTe_2$, Sb_2Te_3, structural transitions

Introduction

Among various techniques of manipulating quantum mechanical effects in materials, strain engineering has emerged as a powerful and versatile tool. In this field, layered materials, characterized by covalently bonded layers held together by weak van der Waals (vdW) forces, have become particularly promising. Applications vary from microchip production (Benck et al. 2014; Gao et al. 2013; Li et al. 2019; Pan et al. 2019; Wang et al. 2014) to supercapacitors and phase-change memory devices (Lee et al. 2020; Mu et al. 2021; Peng et al. 2014; Pumera et al. 2014; Raty, Noé 2020; Wang et al. 2014). The discovery of topological materials (Bernevig et al. 2006; Chen et al. 2009; Kane, Mele 2005a; Konig et al. 2007) with their unique properties has further expanded the horizons of materials science, particularly in the field of straintronics. Topological materials have attracted considerable attention due to their distinctive features. For instance, the inversion of the band gap at an odd number of time-reversed points in the Brillouin zone (Bernevig 2013; Kane, Mele 2005b; Qi, Zhang 2011) leads to interesting properties such as locking the spin momentum of surface states (Singh, Prasad 2016) and the magnetoelectric effect (Tominaga et al. 2015).

In dichalcogenides, monochalcogenides, and certain topological insulators (such as Sb_2Te_3), fine-tuning the properties by altering the interlayer distance appears feasible, due to the strong dependence of the electronic and optical properties on the width of the vdW gap (Fan et al. 2015; Stepanov et al. 2023b; Zhao et al. 2015). As the vdW gap width decreases, a transition from a layered material to a bulk one is expected, leading to radical changes in properties related to structure and non-covalent interactions. However, the anticipated transition from quasi-2D to 3D may not occur (Stepanov et al. 2023a). Therefore, it is crucial to elucidate how noncovalent interactions are distributed during the disruption of the vdW gap and how it affects the geometry and properties of the new phase.

Due to the small band gap in Sb_2Te_3 and $MoTe_2$, metallization is expected to occur before the structural phase transition. Indeed, for both Sb_2Te_3 and $MoTe_2$, external hydrostatic pressure can lead to isostructural phase transitions (IPT), often resulting in anomalies in mechanical, electrical, thermodynamic, and vibrational properties (Bera et al. 2020; Zhao et al. 2015). In this context, interlayer interaction plays a pivotal role; it has been reported that neglecting vdW may lead to the erroneous conclusion that no IPT occurs in the material (Gomis et al. 2011; Zhao et al. 2015). Studying the influence of uniaxial pressure can contribute to a better understanding of the role of vdW interaction in this process.

In this study, in order to generalize and identify patterns in the transformation of non-covalent interactions in layered materials under uniaxial compression, we examine the structure and properties of the representatives of the most promising layered materials ($MoTe_2$ dichalcogenides and Sb_2Te_3 topological insulators). Another important aspect of the study is to consider the influence of non-covalent interactions on the structure after the phase transition and how it affects the IPT.

Computational details

Calculations were performed using the CASTEP quantum chemistry package (Clark et al. 2005). The generalized gradient approximation (GGA) with the Perdew-Burke-Ernzerhof (PBE) parameterization (Ernzerhof, Scuseria 1999) with vdW corrections, important for describing interaction between the layers, was used. The vdW interactions were taken into account using the Grimme method (Grimme 2006; Grimme et al. 2010; 2011). The k space integrals and plane wave basis sets were chosen to ensure total energy convergence at 1 meV/atom. It was found that a kinetic energy cut-off of 500 eV is sufficient for all calculations. Two-Point Steepest Descent (TPSD) algorithm was chosen for the optimization in CASTEP. Such algorithm had previously (Barzilai, Borwein 1988) showed computational structures in best agreement with experimental ones, especially with the application of pressure. Pressure modeling was carried out using uniaxial pressure along the c axis of conventional cells. To carry out relaxation, the structures were optimized at a pressure of 0 GPa.

To study the bonds in phases under pressure, the electron density difference analysis (CDD) was used. For a more detailed study of the vdW interaction, the CRITIC2 code was used (Otero-de-la-Roza et al. 2009; 2014), in which the analysis of the electron density gradient (RDG) between molecular fragments (Johnson et al. 2010) was used to assess their strength.

Results

For the first investigated material, $MoTe_2$ (Fig. 1 (a, b)), as the applied uniaxial pressure increases up to 37 GPa, the valence angle decreases, but the overall structure remains unchanged. However, at a pressure of 37 GPa, a significant transformation occurs as the vdW gap collapses due to the formation of metal-chalcogen bonds through the gap. Simultaneously, based on the CDD analysis, it is observed that covalent bonds perpendicular to the Z axis are disrupted, leading to the rotation of the vdW gap and its reorientation along the Z axis (refer to Fig. 1 (c, d)). It is noteworthy that during this rearrangement, both molybdenum and tellurium maintain coordination consistent with the original structure, albeit violating the octet rule. With an even greater increase in pressure, a lateral displacement of the layers relative to each other occurs. A similar result was also observed for PbS_2 in (Lei et al. 2020).

Fig. 2 illustrates the band structures of $MoTe_2$ under varying pressures. Initially, under uniaxial pressure, the band gap is an indirect gap between the maximum of the valence band (VB) at point Γ and the minimum of the conduction band (CB), located between G- and K-points (Fig. 2 (c)). Upon closer examination, it becomes apparent that the band gap gradually decreases and approaches zero with increasing pressure, attributed to a reduction in the interlayer distance. Band overlap starts at 10 GPa between the top of the valence band and the bottom of the CB (Fig. 2 (e)). Our calculations align with experimental

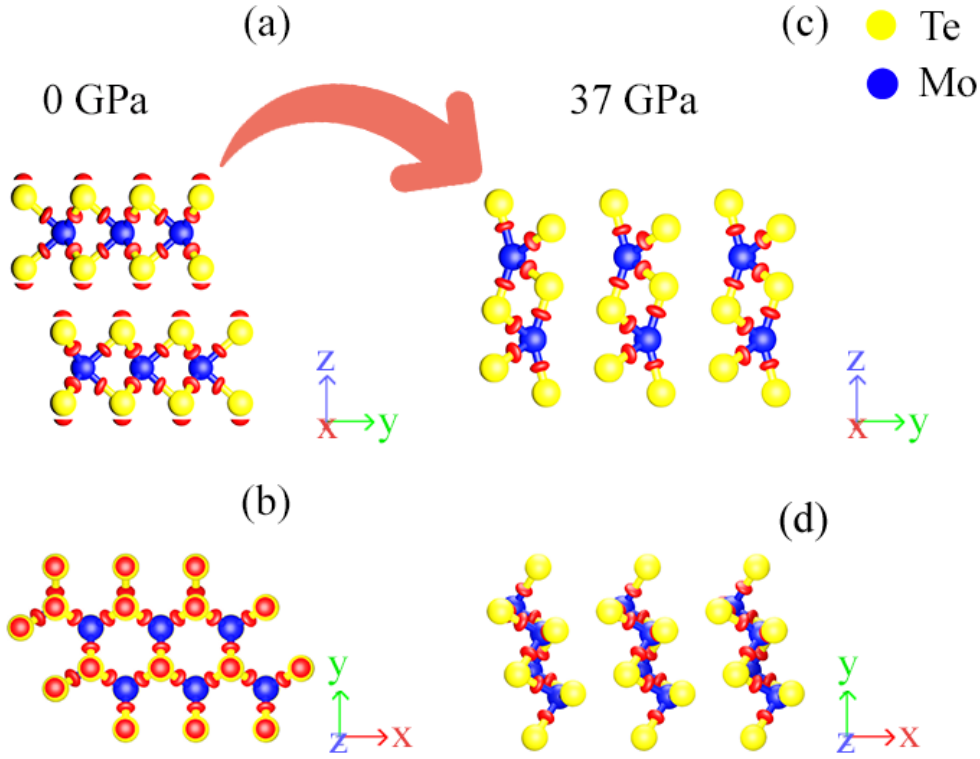

Fig. 1. Transformation of the $MoTe_2$ structure under the influence of axial pressure: (a)–(b) Initial structure (side and top view respectively), (c)–(d) New phase at 37 GPa (side and top view respectively)

measurements, where the onset of metallization occurs at a hydrostatic pressure of 9.6 GPa (Zhao et al. 2019).

With pressure increase, both the CB and VB experience energy shifts due to enhanced interlayer electronic coupling. At a pressure of 20 GPa (Fig. 2 (f)), the CB minimum and VB maximum intersect the Fermi level, signifying metallization. Importantly, the cell symmetry remains unchanged, indicating an IPT. Similar to other TMDs, pressure-induced shifts of extremes generate a series of electron and hole pockets. Given the larger atomic radius of Te and wider electron orbitals compared to Se and S, this may contribute to $MoTe_2$ achieving metallization at a lower pressure than most other TMDs such as MoS_2, $MoSe_2$, and WS_2.

As already mentioned, under pressure, the $MoTe_2$ structure does not change coordination when transitioning to a new phase and it may resemble the relaxed GaSe structure. In our previous work (Stepanov et al. 2023a), it was established that in monochalcogenides the vdW gap closes under the action of applied uniaxial pressure. Analysis of the CDD distribution revealed the formation of quasi-one-dimensional chains with non-covalent interactions between them. In this work, during the relaxation of the structure in Fig. 3 (b), it is found that the original 0 GPa phase in Fig. 3 (a) is not restored. Instead, a distortion of the 14 GPa phase occurs, which leads to a transition from chains with non-covalent interactions between them to a two-dimensional structure, albeit with an orthogonally reoriented vdW gap (Fig. 3 (c)). It is important to note that the atomic coordination returns to its original state, breaking the octet rule. Thus, both $MoTe_2$ and GaSe have in common the fact that in these materials it is possible to achieve reorientation of the vdW gap while maintaining coordination.

RDG analysis was used to confirm vdW gap reorientation in these materials. Figs. 4 (a, b) shows structures with a reoriented vdW gap for relaxed GaSe and $MoTe_2$ under pressure. Isosurface between layers indicates the presence of non-covalent interactions between layers. In the case of GaSe, under uniaxial pressure, a redistribution of interactions occurs, which determines the chain structure. A more detailed study of the connections between chains is the subject of our further research. During the relaxation process, the material again becomes quasi-two-dimensional and the vdW surface is restored again.

 https://www.doi.org/10.33910/2687-153X-2024-5-1-30-38

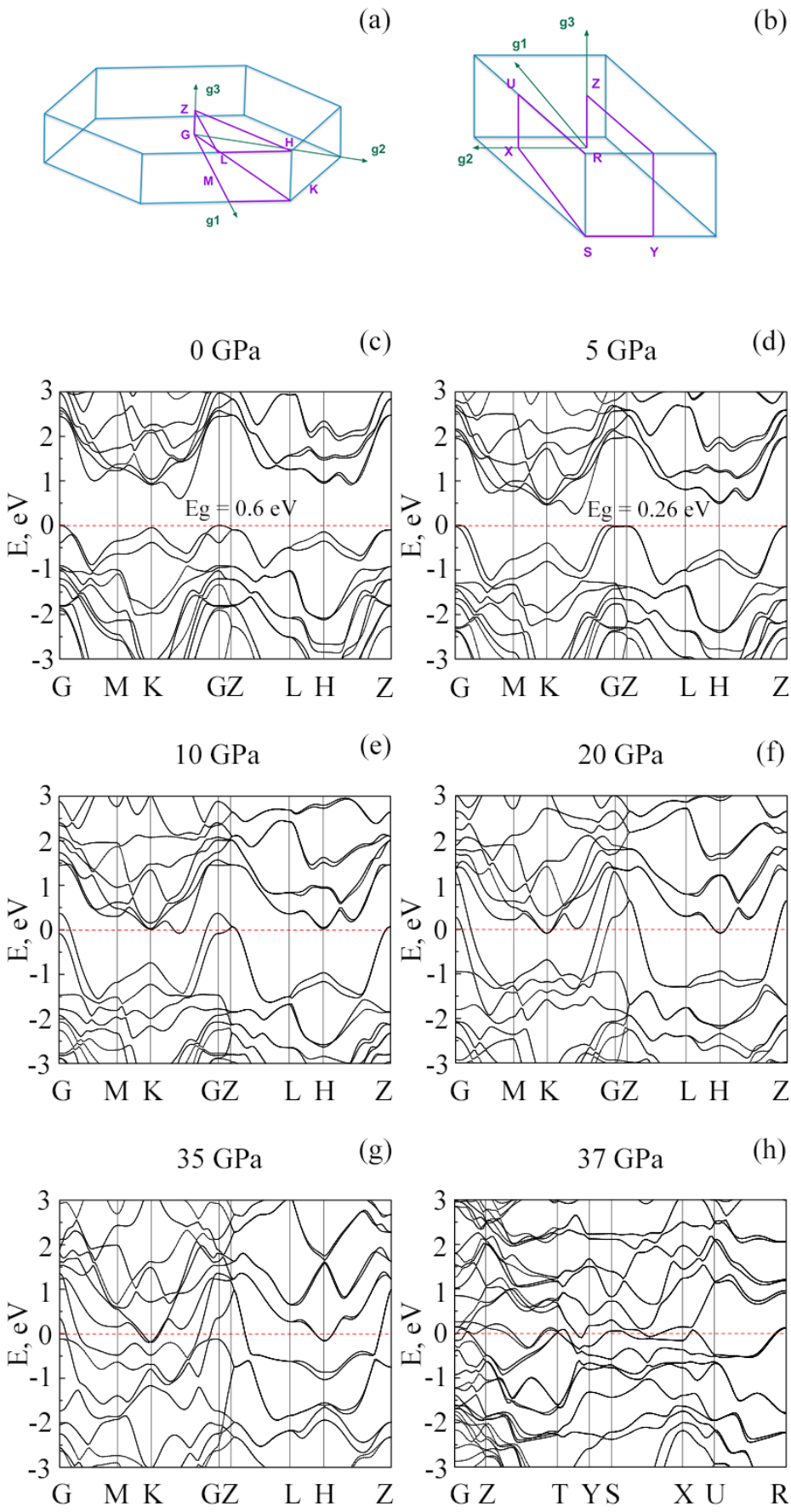

Fig. 2. Band structure patterns for $MoTe_2$ under different uniaxial pressures. (a)–(b) Brillouin zones for two phases (0 and 37 GPa). (c)–(h) Band structures for different pressure values

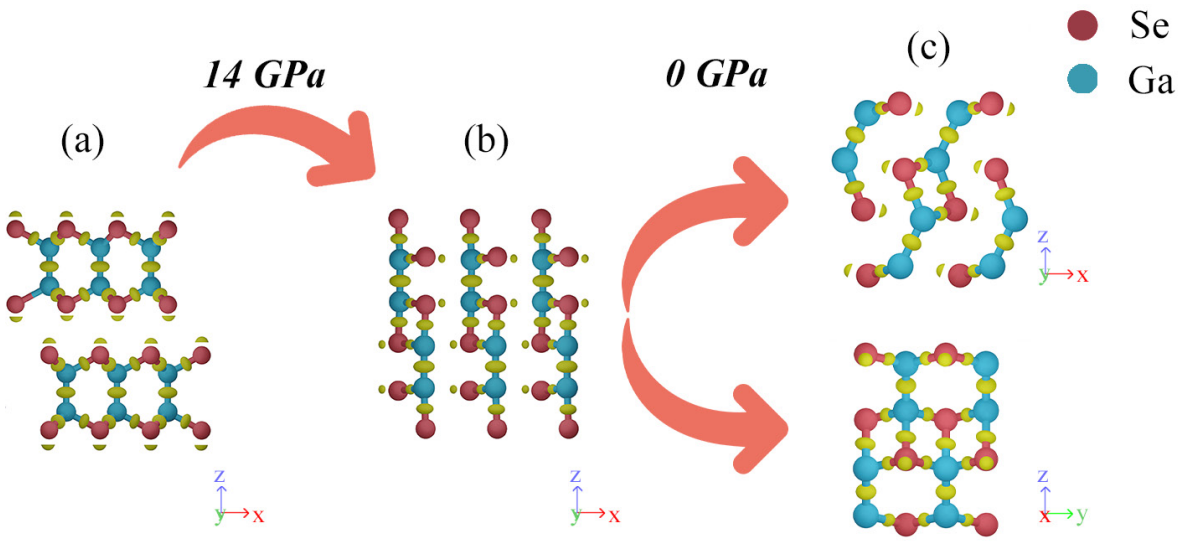

Fig. 3. Transformation of the GaSe structure under the influence of axial pressure and after releasing the pressure. (a) Initial structure, (b) New phase at 14 GPa, and (c) at a pressure of 0 GPa. Yellow balls represent CDD clouds

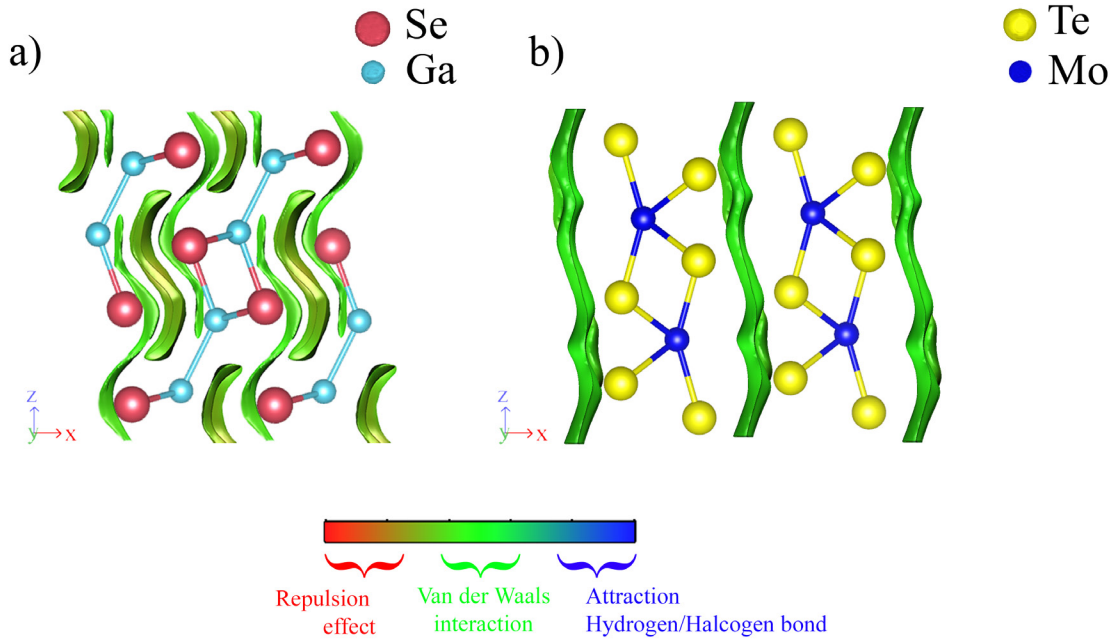

Fig. 4. RDG analysis of relaxed GaSe and $MoTe_2$ under pressure. Green isosurface shows the areas of vdW interaction

All of the above-mentioned classes of materials have one important common characteristic: the formation of a vdW gap, caused by additional CDD clouds associated with partial sp^3 hybridization of chalcogen atoms. Consequently, materials with similar CDD distributions are expected to exhibit similar vdW gap reconstruction patterns. For example, in graphite, which is known for the lack of additional density in the vdW gap, changes under pressure are significantly different. As for Sb_2Te_3, additional clouds of electron density in the gap are also observed in this material (Fig. 5 (a)). Despite that in the case of other materials (Figs. 1 and 3) these clouds undergo the transition to the new phase, but in the case of antimony telluride they retain their configuration and location in the new phase. Moreover, the question of the nature of interlayer interaction in Sb_2Te_3 remains unanswered, and there are reports that the connection between layers may be metavalent in nature (Zhang et al. 2023).

 https://www.doi.org/10.33910/2687-153X-2024-5-1-30-38

Under uniaxial pressure, antimony telluride undergoes a transition to a metallic state while preserving its layered structure. A further increase in pressure leads to a strong lateral displacement of the layers and a phase transition at 7 GPa (Fig. 5 (c)). In this case, the vdW gap disappears in the new phase. However, it is crucial to note that there are no bonds between the atoms through the gap; they possess lone pairs and engage in non-covalent interactions. Consequently, the closure of the gap is linked to the lateral sliding of the layers relative to each other along the vdW gap. This is distinct from the rearrangement of bonds seen in other layered materials.

When compared, the results at different pressures make it apparent that the impact of pressure on Sb_2Te_3 is mirrored in the band structure: bands at higher pressures exhibit slight broadening compared to those at lower pressures (Fig. 6 (c, d)). This aligns with heightened interactions between neighboring atoms, electrons, and orbitals resulting from a decreased interlayer distance.

Between pressures of 0 to 3 GPa (Fig. 6 (c, d)), the conduction band minimum (CBM) sharply decreases between points Γ and Z. The Valence Band Maximum (VBM) undergoes significant positional changes with pressure increase: at 0 GPa, it resides at point Γ, and with increasing pressure, it shifts from point Γ along the path to point M. By 3 GPa (Fig. 6 (d)), the CBM crosses the Fermi level, signifying metallization (Fig. 6 (e, f)) without undergoing a phase transition.

CDD analysis of the initial structures shows that the mechanism of interlayer interaction for all materials studied is determined to a large extent by the interaction between permanent dipoles, represented by the additional electron density in the vdW gap. When pressure is applied, all materials under study demonstrate different patterns of change in the vdW gap. In Sb_2Te_3, bonds inside the layer are not broken, and bonds through the gap arise due to the lateral displacement of the layers, without forming a vdW interaction plane, but creating regions with vdW interaction due to lone electron pairs.

At the same time, for GaSe and $MoTe_2$, the bonds inside the layer between the metal and chalcogen atoms are broken and arise through the vdW gap. Two-dimensional layers appear in $MoTe_2$, and quasi-one-dimensional chains appear in GaSe, and the symmetry of the cell in both these cases changes from hexagonal to orthorhombic. When GaSe relaxes, the symmetry does not increase and two-dimensional layers are formed with an orientation similar to the case of $MoTe_2$ (under pressure).

This leads to an important point: the vdW interaction does not disappear when axial pressure is applied. From the presented results it is obvious that, depending on the magnitude of intralayer interaction, coordination and local symmetry, the vdW gap can either rearrange ($MoTe_2$ and GaSe) or distribute, forming regions of non-covalent interaction, as seen in the example of Sb_2Te_3.

During relaxation of Sb_2Te_3, the regions of non-covalent interaction, due to an increase in symmetry, are united again into a single vdW surface. This result is consistent with the work of (Zheng et al. 2023),

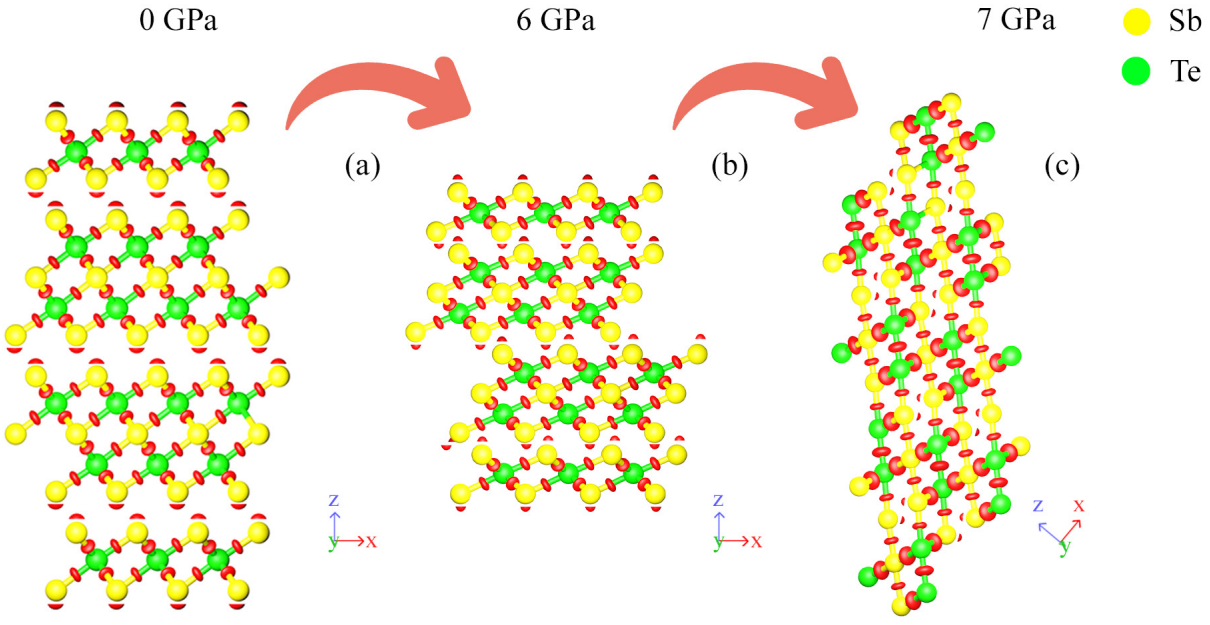

Fig. 5. Transformation of the Sb_2Te_3 structure under the axial pressure. (a) Initial structure, (b) Structure at 6 GPa before the phase transition, (c) New phase at 7 GPa. Red balls represent CDD clouds

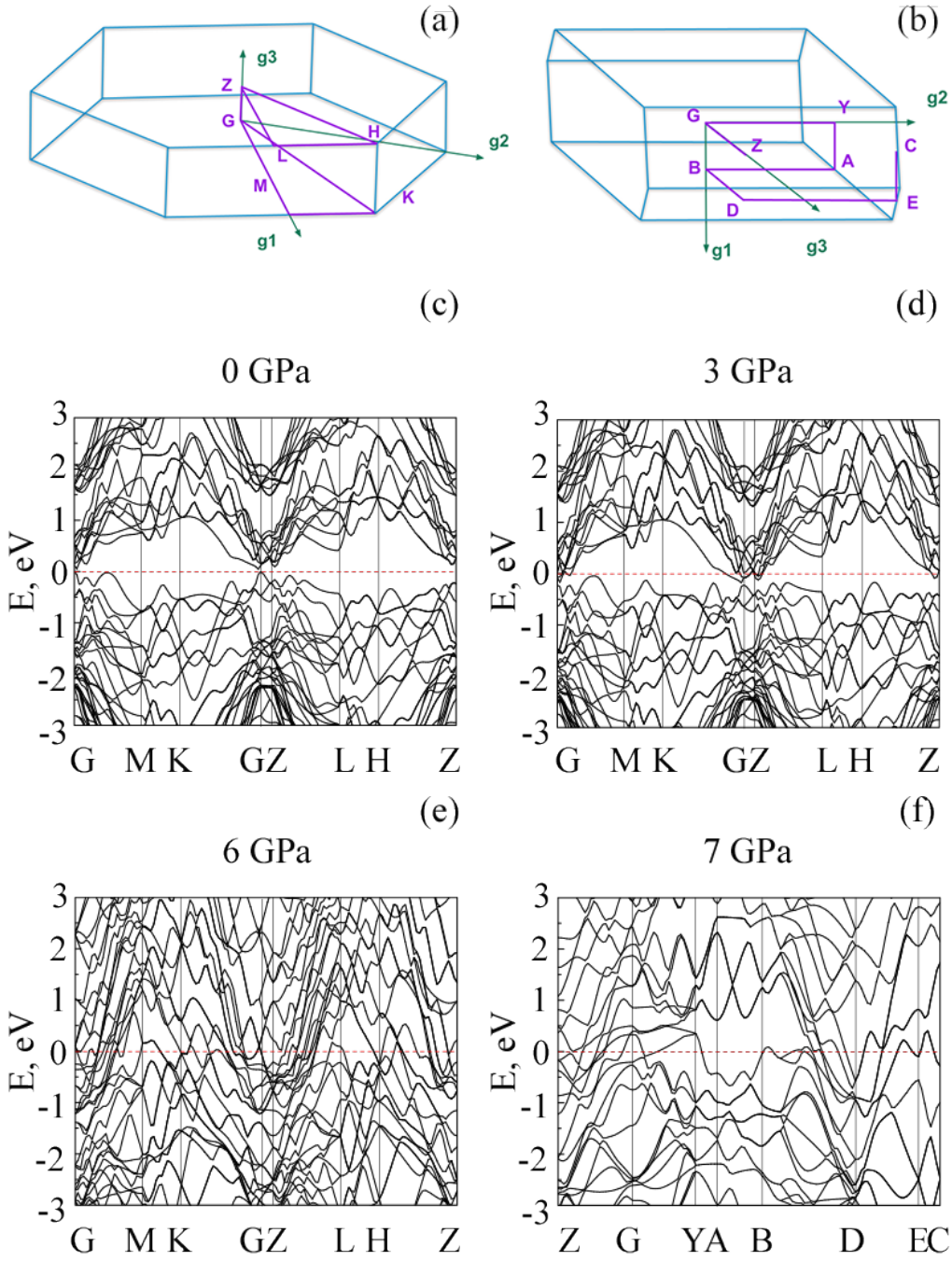

Fig. 6. Band structure patterns for Sb_2Te_3 under different uniaxial pressures. (a)–(b) Brillouin zones for two phases of Sb_2Te_3 (0 and 7 GPa). (c)–(e) Band structures for different pressure values

where it was shown that during the crystallization of Sb_2Te_3, the vdW gap is formed from vacancies (or, as we called it here, non-covalent interaction regions), which are pushed out in a correlated manner, forming a single defective surface — vdW surface.

Conclusions

It was shown that in $MoTe_2$, as in Sb_2Te_3, an isostructural phase transition associated with metallization occurs. It is shown that at a pressure of 37 GPa, a restructuring occurs in $MoTe_2$ with a change in the orientation of the vdW gap. Similar behavior is observed for the relaxed GaSe structure. For antimony telluride, the mechanism turned out to be different — it is associated with the redistribution of non-covalent interaction under the influence of axial pressure. In Sb_2Te_3, a phase transition occurs with

 https://www.doi.org/10.33910/2687-153X-2024-5-1-30-38

a change in symmetry due to the lateral sliding of the layers relative to each other, as a result of which a bulk structure with regions of non-covalent interaction is formed. It turned out that the symmetry and bond strength inside the layer play a significant role. Thus, it becomes possible to distinguish two mechanisms of destruction and formation of the vdW gap — with reconfiguration of the gap and redistribution of non-covalent interaction.

Conflict of Interest

The author declares that there is no conflict of interest, either existing or potential.

Acknowledgements

Author would like to express his sincere gratitude to Vasilisa Gerega, Anton Suslov, and Alexander Kolobov. Author is deeply appreciative of their insights, guidance, and comments, which have played a pivotal role in the successful completion of this work.

References

Barzilai, J., Borwein, J. M. (1988) Two-point step size gradient methods. *IMA Journal of Numerical Analysis*, 8(1), 141–148. https://doi.org/10.1093/imanum/8.1.141 (In English)

Benck, J. D., Hellstern, T. R., Kibsgaard, J. et al. (2014) Catalyzing the hydrogen evolution reaction (HER) with molybdenum sulfide nanomaterials. *Acs Catalysis*, 4 (11), 3957–3971. https://doi.org/10.1021/cs500923c (In English)

Bera, A., Singh, A., Gupta, S. N. et al. (2020) Pressure-induced isostructural electronic topological transitions in 2H-$MoTe_2$: X-ray diffraction and first-principles study. *Journal of Physics: Condensed Matter*, 33 (6), article 065402. https://doi.org/10.1088/1361-648X/abaeac (In English)

Bernevig, B. A. (2013) *Topological insulators and topological superconductors*. Princeton: Princeton University Press, 260 p. (In English)

Bernevig, B. A., Hughes, T. L., Zhang, S. C. (2006) Quantum spin Hall effect and topological phase transition in HgTe quantum wells. *Science*, 314 (5806), 1757–1761. https://www.science.org/doi/10.1126/science.1133734 (In English)

Chen, Y. L., Analytis, J. G., Chu, J.-H. et al. (2009) Experimental realization of a three-dimensional topological insulator, Bi_2Te_3. *Science*, 325 (5937), 178–181. https://doi.org/10.1126/science.1173034 (In English)

Clark, S. J., Segall, M. D., Pickard, C. J. et al. (2005) First principles methods using CASTEP. *Zeitschrift für Kristallographie-Crystalline Materials*, 220 (5-6), 567–570. https://doi.org/10.1524/zkri.220.5.567.65075 (In English)

Ernzerhof, M., Scuseria, G. E. (1999) Assessment of the Perdew–Burke–Ernzerhof exchange-correlation functional. *The Journal of Chemical Physics*, 110 (11), 5029–5036. https://doi.org/10.1063/1.478401 (In English)

Fan, X., Chang, C.-H., Zheng, W. T. et al. (2015) The electronic properties of single-layer and multilayer MoS_2 under high pressure. *The Journal of Physical Chemistry C*, 119 (19), 10189–10196. https://doi.org/10.1021/acs.jpcc.5b00317 (In English)

Gao, M.-R., Xu, Y.-F., Jiang, J., Yu, S.-H. (2013) Nanostructured metal chalcogenides: Synthesis, modification, and applications in energy conversion and storage devices. *Chemical Society Reviews*, 42 (7), 2986–3017. https://doi.org/10.1039/C2CS35310E (In English)

Grimme, S. (2006) Semiempirical GGA-type density functional constructed with a long-range dispersion correction. *Journal of Computational Chemistry*, 27 (15), 1787–1799. https://doi.org/10.1002/jcc.20495 (In English)

Grimme, S., Antony, J., Ehrlich, S., Krieg, H. (2010) A consistent and accurate ab initio parametrization of density functional dispersion correction (DFT-D) for the 94 elements H-Pu. *The Journal of Chemical Physics*, 132 (15). https://doi.org/10.1063/1.3382344 (In English)

Grimme, S., Ehrlich, S., Goerigk, L. (2011) Effect of the damping function in dispersion corrected density functional theory. *Journal of Computational Chemistry*, 32 (7), 1456–1465. https://doi.org/10.1002/jcc.21759 (In English)

Johnson, E. R., Keinan, S., Mori-Sánchez, P. et al. (2010) Revealing noncovalent interactions. *Journal of the American Chemical Society*, 132 (18), 6498–6506. https://doi.org/10.1021/ja100936w (In English)

Kane, C. L., Mele, E. J. (2005a) Quantum spin Hall effect in graphene. *Physical Review Letters*, 95 (22), article 226801. https://doi.org/10.1103/PhysRevLett.95.226801 (In English)

Kane, C. L., Mele, E. J. (2005b) Z_2 topological order and the quantum spin Hall effect. *Physical Review Letters*, 95 (14), article 146802. https://doi.org/10.1103/PhysRevLett.95.146802 (In English)

Konig, M., Wiedmann, S., Brune, C. et al. (2007). Quantum spin Hall insulator state in HgTe quantum wells. *Science*, 318 (5851), 766–770. https://doi.org/10.1126/science.1148047 (In English)

Lee, E., Kim, J., Bhoyate, S. et al. (2020) Realizing scalable two-dimensional MoS_2 synaptic devices for neuromorphic computing. *Chemistry of Materials*, 32 (24), 10447–10455. https://doi.org/10.1021/acs.chemmater.0c03112 (In English)

Lei, W., Wang, W., Ming, X. et al. (2020) Structural transition, metallization, and superconductivity in quasi-two-dimensional layered PdS2 under compression. *Physical Review B*, 101 (20), article 205149. https://doi.org/10.1103/PhysRevB.101.205149 (In English)

Li, P., Yuan, K., Lin, D.-Y. et al. (2019) p-MoS_2/n-InSe van der Waals heterojunctions and their applications in all-2D optoelectronic devices. *RSC Advances*, 9 (60), 35039–35044. https://doi.org/10.1039/C9RA06667E (In English)

Mu, C., Sun, X., Chang, Y. et al. (2021) High-performance flexible all-solid-state micro-supercapacitors based on two-dimensional InSe nanosheets. *Journal of Power Sources*, 482, article 228987. https://doi.org/10.1016/j.jpowsour.2020.228987 (In English)

Otero-de-la-Roza, A., Blanco, M. A., Pendás, A. M., Luaña, V. (2009) Critic: A new program for the topological analysis of solid-state electron densities. *Computer Physics Communications*, 180 (1), 157–166. https://doi.org/10.1016/j.cpc.2008.07.018 (In English)

Otero-de-la-Roza, A., Johnson, E. R., Luaña, V. (2014) Critic2: A program for real-space analysis of quantum chemical interactions in solids. *Computer Physics Communications*, 185 (3), 1007–1018. https://doi.org/10.1016/j.cpc.2013.10.026 (In English)

Pan, H., Cao, L., Chu, H. et al. (2019) Broadband nonlinear optical response of InSe nanosheets for the pulse generation from 1 to 2 μm. *ACS Applied Materials & Interfaces*, 11 (51), 48281–48289. https://doi.org/10.1021/acsami.9b18632 (In English)

Peng, X., Peng, L., Wu, C., Xie, Y. (2014) Two dimensional nanomaterials for flexible supercapacitors. *Chemical Society Reviews*, 43 (10), 3303–3323. https://doi.org/10.1039/C3CS60407A (In English)

Pumera, M., Sofer, Z., Ambrosi, A. (2014) Layered transition metal dichalcogenides for electrochemical energy generation and storage. *Journal of Materials Chemistry A*, 2 (24), 8981–8987. https://doi.org/10.1039/C4TA00652F (In English)

Qi, X.-L., Zhang, S.-C. (2011) Topological insulators and superconductors. *Reviews of Modern Physics*, 83 (4), article 1057. https://doi.org/10.1103/RevModPhys.83.1057 (In English)

Raty, J.-Y., Noé, P. (2020) Ovonic threshold switching in Se-Rich Ge_xSe_{1-x} glasses from an atomistic point of view: The crucial role of the metavalent bonding mechanism. *Physica Status Solidi (RRL)*, 14 (5), article 1900581. https://doi.org/10.1002/pssr.201900581 (In English)

Singh, B., Prasad, R. (2016) Spin-texture of the non-trivial surface state of topological insulator Sb_2Te_3. *Quantum Matter*, 5 (3), 362–364. https://doi.org/10.1166/qm.2016.1317 (In English)

Stepanov, R., Gerega, V., Suslov, A., Kolobov, A. (2023a) Uniaxial pressure-induced 2D–1D dimensionality change in GaSe and related materials. *Physica Status Solidi (RRL)*, 17 (8), article 2200430. https://doi.org/10.1002/pssr.202200430 (In English)

Stepanov, R. S., Marland, P. I., Kolobov, A. V. (2023b) Compositional and structural disorder in two-dimensional $A^{III}B^{VI}$ materials. *Crystals*, 13 (8), article 1209. https://doi.org/10.3390/cryst13081209 (In English)

Tominaga, J., Kolobov, A. V., Fons, P. J. et al. (2015) Giant multiferroic effects in topological GeTe-Sb_2Te_3 superlattices. *Science and Technology of Advanced Materials*, 16 (1), article 014402. https://doi.org/10.1088/1468-6996/16/1/014402 (In English)

Wang, H., Feng, H., Li, J. (2014) Graphene and graphene-like layered transition metal dichalcogenides in energy conversion and storage. *Small*, 10 (11), 2165–2181. https://doi.org/10.1002/smll.201303711 (In English)

Zhao, K., Wang, Y., Sui, Y. et al. (2015) First principles study of isostructural phase transition in Sb_2Te_3 under high pressure. *Physica Status Solidi (RRL)*, 9 (6), 379–383. https://doi.org/10.1002/pssr.201510091 (In English)

Zhao, X.-M., Liu, H.-Y., Goncharov, A. F. et al. (2019) Pressure effect on the electronic, structural, and vibrational properties of layered 2H – $MoTe_2$. *Physical Review B*, 99 (2), article 024111. https://doi.org/10.1103/PhysRevB.99.024111 (In English)

Zheng, Y., Song, W., Song, Z. et al. (2023) A complicated route from disorder to order in antimony-tellurium binary phase change materials. *Advanced Science*, article 2301021. https://doi.org/10.1002/advs.202301021 (In English)